# Investigation of Nitrogen Doping Effects on the Performance of Graphene in Lithium-Ion Batteries Using Density Functional Theory

Mohammed Abdulhussain Al-Kaabi and Worood S. Rasool
*Department of Physics, College of Science, Kerbala University, 56001 Karbala, Iraq*
*mohammed.alkaabi@uokerbala.ed.iq, worood.s@s.uokerbala.edu.iq*

Keywords: Graphene, Lithium-Ion Batteries, Doping N-Defect Graphene, Anode Materials, DFT.

Abstract: We performed first-principles calculations using density functional theory (DFT) with the CASTEP code in Materials Studio to investigate the adsorption behaviour of lithium (Li) on graphene featuring single defects. Our study employed the generalized gradient approximation (GGA-PBE) to analyse the adsorption and diffusion characteristics of Li on three distinct graphene structures: pristine graphene, graphitic nitrogen-doped graphene (NG), and pyridinic nitrogen-doped graphene (NG1). The results indicated that Li diffusion occurs significantly faster on N-doped graphene compared to pristine graphene. Specifically, the calculated diffusion energy barriers were found to be 0.82 eV for pristine graphene, 1.83 eV for NG, and 0.65 eV for NG1. This suggests that NG1, with its lower energy barrier, facilitates Li movement more efficiently than the other structures. Furthermore, NG1 demonstrated a remarkable theoretical specific capacity of 453.88 mAh/g, underscoring its potential as an advanced anode material for lithium-ion batteries (LiBs). Overall, our findings highlight that nitrogen-doped defect graphene not only improves lithium diffusion kinetics but also enhances the overall capacity for lithium storage, making it a highly promising candidate for next-generation LiB applications.

## 1 INTRODUCTION

In recent years, lithium-ion batteries (LIBs) have gained considerable attention due to their high energy density and excellent efficiency. Consequently, they are widely used in portable electronic devices, including smartphones, tablets, laptops and other mobile gadgets [1]. LIBs are regarded as one of the most promising energy storage technologies, owing to their advantages such as high efficiency, compact size, lightweight nature, temperature responsiveness, and ease of maintenance [2].

Among various anode materials, graphite remains the most widely used option, boasting a specific capacity of 372 mAh/g [3]. Carbon is a versatile element, forming structures that encompass a range of dimensionalities in nature. Until a few decades ago, only three carbon allotropes were commonly recognized: graphite, diamond and amorphous carbon [4].

Graphene, a single layer of graphite, can be isolated from bulk material or synthesized as a monolayer. Its carbon atoms are arranged in a flat, sheet-like hexagonal lattice, forming a honeycomb pattern with a bond angle of 120° and an interatomic distance of 1.42 Å [5]. As a two-dimensional (2D) $sp^2$-hybridized carbon allotrope, graphene has attracted immense interest due to its unique electronic properties, such as the half-integer quantum Hall effect, high electron mobility, and massless Dirac fermions [6]. The successful isolation of graphene by Andre Geim and Konstantin Novoselov at the University of Manchester in 2004 sparked a surge of global research interest [7]. Since then, numerous studies have explored its potential applications as an anode material for LIBs [8]-[13].

This growing interest is driven by graphene's ability to adsorb lithium on both surfaces, with its available surface area for lithium storage far exceeding the interlayer spacing of graphite. Its flat, monolayer structure facilitates rapid lithium diffusion, making graphene a prominent subject in theoretical investigations as a prospective anode material for LIBs [14]-[17].

Moreover, doped graphene has been successfully synthesized, with nitrogen-doped (N-doped) graphene initially produced using the chemical vapor deposition (CVD) method [18]. Recent developments have introduced various innovative techniques for fabricating N-doped graphene [19], [20].

Investigations into N-doped graphene as an anode material for LIBs highlight several advantages [21]. Extensive research indicates that N-doped graphene is a promising anode candidate, primarily due to the higher electronegativity of nitrogen compared to carbon and the hybridization between nitrogen's lone pair electrons and the graphene lattice [22].

In this study, we investigate lithium (Li) diffusion across a graphene monolayer using density functional theory (DFT) calculations. We find that the diffusion energy barrier for pristine graphene is significantly high. To lower this barrier, we examine Li diffusion through graphene containing commonly observed defects. The energy barriers for doped graphene with single defects are also calculated, revealing that such defects reduce the diffusion barriers.

# 2 COMPUTATIONAL DETAILS

Since the formulation of two foundational theorems by Hohenberg and Kohn in 1964 [23], density functional methods have grown increasingly popular over the past decade [24]. These theorems assert that the ground state energy of a system is determined by a unique electron density functional, under the assumption that the "true" computed density minimizes the system's total energy. A practical approach to obtaining this density was subsequently introduced by Kohn and Sham, involving an iterative solution of single-electron wave equations. This approach incorporates three key potentials: exchange-correlation effects, coulomb repulsion among electrons and other particles in the system, and interactions between electrons and nuclei [25]. As the goal is to determine the ground-state electron density, Kohn and Sham showed that the complex many-body Schrödinger equation could be simplified to a single-electron (1), [26].

$$\left[\frac{h^2}{2m}\nabla^2 + V(\mathbf{r}) + V_H(\mathbf{r}) + V_{\mathrm{XC}}(\mathbf{r})\right]\psi_i(\mathbf{r}) = \varepsilon_i\psi_i(\mathbf{r}) \quad (1)$$

The Kohn–Sham equation yields single-electron wave functions, each dependent on only three spatial coordinates. The potential $V$ on the left-hand side of the Kohn–Sham equation represents the interaction between an individual electron and a set of atomic nuclei.

CASTEP is employed to carry out periodic DFT calculations. The generalized gradient approximation (GGA) exchange-correlation functional developed by Perdew, Burke, and Ernzerhof (PBE) is utilized [27]. The convergence criterion for the electronic self-consistent loop is set to $10^{-6}$ eV, and the wave functions are represented using plane waves with a cutoff energy of 450 eV. Structural relaxation continues until the self-consistent force on each atom is reduced below 0.03 eV/Å $^{-1}$. To eliminate artificial interactions due to periodic boundary conditions, a vacuum spacing of 15 Å is introduced perpendicular to the surface. For Brillouin zone integration, a 3×3×1 Γ-centered Monkhorst–Pack (MP). The N-doped graphene system modeled in this study was assigned a doping concentration of approximately 2.04 at%, which aligns with experimental reports [28]-[30]. To compare the binding strength of Li in graphene-based systems, the adsorption energy ($E_{ad}$) was calculated using the following expression the (2), [31]:

$$E_{ad} = \left(E_{\mathrm{Total}} - E_g - nE_{Li}\right)/n_{Li} \quad (2)$$

Here, $E$ Total represents the total energy of the Li–graphene system, $E$ Li denotes the total energy of an isolated Li atom, $n$ is the number of adsorbed atoms, and Eg corresponds to the total energy of the isolated graphene sheet.

A key parameter for evaluating electrode performance is the theoretical capacity. The theoretical capacity of the material is determined using the (3), [32].

$$Q = 1000 \times F \times z\frac{n}{M_a} \quad (3)$$

In this context, F, z, $n$ , and Ma represent the Faraday constant (F=26.801 Ah/mol), the number of valence electrons (z=1 for Li), the number of intercalated Li ions ($n$), and the molar mass of the host system without the ion ($Ma$) [33].

Surface migration of Li ion on graphene structures ionic conductivity, a critical factor that directly influences the rate performance of LIB electrode materials, is governed by Li ion migration. Rapid Li diffusion plays a vital role in ensuring fast charge–discharge cycles and achieving high power densities in batteries. The study of the diffusion properties and the activation energies of Li adsorbed on the surface was performed with the nudged elastic band method (NEB) [34], [35].

# 3 RESULTS AND DISCUSSION

## 3.1 Graphene Doping with Nitrogen Atom

The computer models of graphene structures are displayed in Figure 1. The two bonding configurations that a nitrogen atom can primarily

exist in within the carbon lattice when doped into graphene are graphitic and pyridinic. To represent graphitic-N (NG) and pyridinic-N (NG1), geometric structures of three potential configurations were constructed and optimized. The pyridinic-N bonding arrangement is stable when a monovacancy is present. NG1 was produced by removing one carbon atom and replacing it with one nitrogen atom, resulting in a mono-vacancy defect. Nitrogen, possessing the electronic configuration $2s^2 2p^3$, introduces three valence electrons to form σ-bonds with neighboring carbon atoms when incorporated into a graphitic nitrogen configuration (NG). A fourth electron delocalizes to participate in π-bonding, while the remaining unpaired electron partially occupies the π* antibonding states within the conduction band [36].

## 3.2 Li Adsorption Sites and Adsorption Energies

To identify the most favorable lithium adsorption site on each graphene-based structure, three possible adsorption configurations were considered, as illustrated in Figure 1 the center of the hexagonal ring (H site), the top of a carbon or dopant atom (T site) and the bridge site above the midpoint of a C–C or C–N bond (B site). The adsorption energy for lithium was calculated using the standard adsorption energy (2) to assess its interaction with doped graphene surfaces. A summary of the computed adsorption energies for each site and structure is presented in Table 1. Notably, although lithium was initially positioned at T, B, and H sites, structural relaxation consistently led to convergence at the H site, indicating its energetic preference. It is important to note that in periodic systems, long-range elastic interactions can introduce energy variations due to the spurious interactions between defects and their periodic images, potentially affecting the calculated adsorption energies. The calculated adsorption energy for the NG1 configuration is -1.24 eV, which is notably more negative than that of pristine (undoped) graphene, recorded at -1.11 eV. This indicates a stronger interaction between lithium atoms and the NG1 surface. The enhanced binding energy can be attributed to the presence of surface dangling bonds formed as a result of vacancy defects, which serve as favorable anchoring sites for lithium adsorption. As a result, Li atoms tend to remain stably positioned at the center of the defect site. Among the investigated adsorption sites, the H site located at the center of the hexagonal ring emerges as the most energetically favorable position for lithium, in agreement with previous studies [37]. The relatively weak interaction between lithium and NG is primarily due to nitrogen high electronegativity (3.04), which attracts electrons from adjacent carbon atoms and reduces Li ability to donate charge in its vicinity. This electron-rich environment causes Li to shift away from the nitrogen site after adsorption. In contrast, although NG1 also contains nitrogen, the presence of vacancy-induced defects enhances Li binding by offering unsaturated, reactive sites. Figure 2 displays the optimized geometries of Li adsorption on graphene, NG, and NG1, along with the nearest atomic distances. In all cases, Li is initially positioned approximately 1.251 Å above the graphene plane.

## 3.3 Surface Migration of Li Ions on Graphene Structures

The diffusion energy barriers for lithium migration were evaluated across all investigated graphene-based structures. To enable a consistent comparison, we focused on the minimum energy barriers along diffusion pathways leading to the most energetically favorable adsorption sites. Figures 3, 4, and 5 illustrate the calculated diffusion energy barriers and the corresponding migration paths. For pristine graphene, the diffusion energy barrier was calculated to be 0.82 eV, aligning well with values previously reported in the literature [37]. Among the doped structures, NG1 demonstrated the most favorable lithium diffusion behavior, with a significantly lower energy barrier of approximately 0.65 eV (see Table 2). This enhanced mobility can be attributed to electron–electron repulsion between the dopant atom and the lithium ion, which tends to push Li away from the nitrogen site and toward energetically preferred adsorption positions. In contrast, NG exhibited a relatively higher diffusion barrier of approximately 1.83 eV. This is largely due to the influence of nitrogen doping, which eliminates carbon-centered radicals near defect sites and thereby hinders lithium migration [38]. Despite these variations, all structures maintained acceptable ionic conductivity with manageable energy barriers along their respective migration pathways.

Table 1: The most stable location for Li adsorption, and the adsorption energy ($E_{ad}$).

| Structure | Most stable adsorption site | Adsorption energy(eV) | Theoretical studies [22] | Distance(Å) |
|---|---|---|---|---|
| Graphene | H | -1.11 | -0.98 | 2.251 |
| NG | $H_1$ | -1.12 | -0.95 | 2.211 |
| NG1 | $H_2$ | -1.24 | -1.37 | 2. 171 |

Table 2: The diffusion barrier height $\Delta E_b$(eV).

| Structure | Diffusion barrier height ΔEb(eV) |
|---|---|
| Graphene | 0.82 |
| NG | 1.83 |
| NG1 | 0.65 |

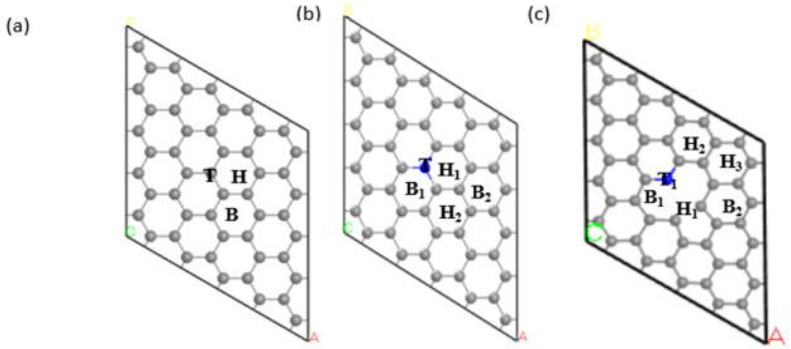


Figure 1: Optimized structures of a) graphene, b) NG, c) NG1.

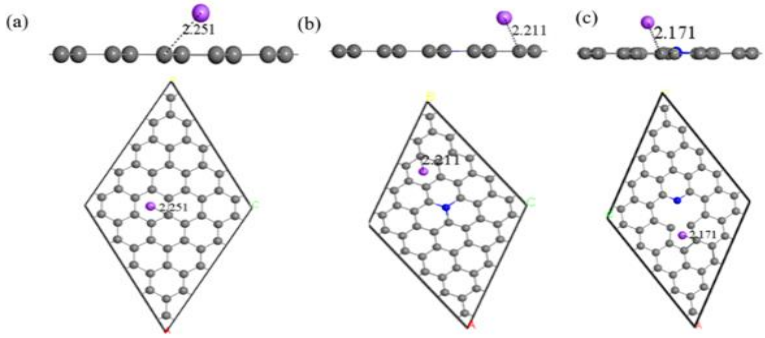


Figure 2: Optimized interaction geometry of Li and a) graphene, b) NG, c) NG1.

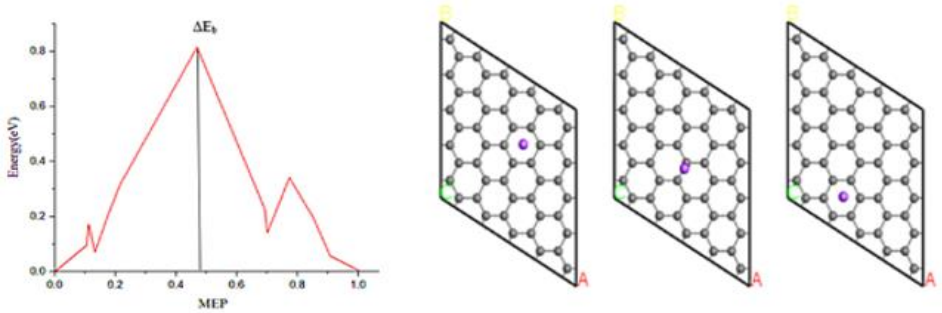


Figure 3: The energy barrier ($\Delta E_b$) for graphene.

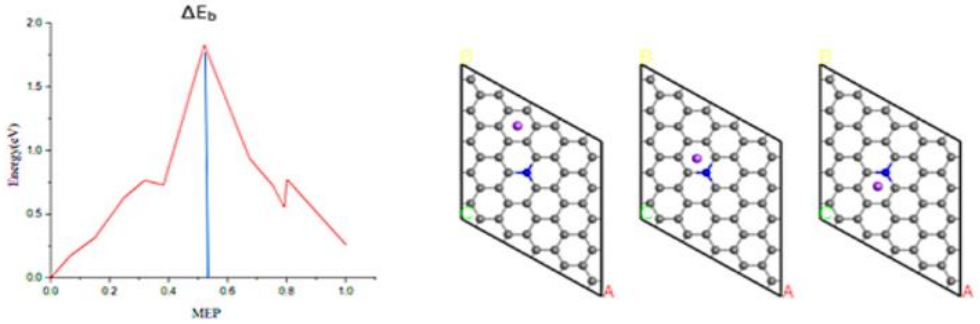


Figure 4: The energy barrier (ΔEb) for NG.

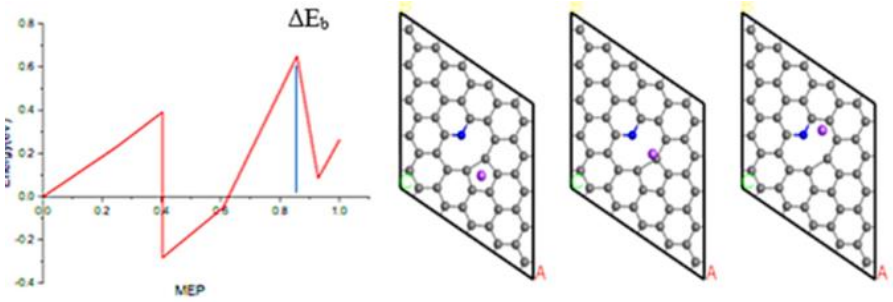


Figure 5: The energy barrier ($\Delta E_b$) for NG1.

## 3.4 Theoretical Capacity

The lithium storage capacity of an anode material is a critical parameter in determining its applicability for lithium-ion batteries (LiBs). To further elucidate the lithium storage mechanism in heteroatom-doped defect graphene, the structural configuration of lithium atoms was analyzed. Figure 6 illustrates the optimized geometry of ten lithium atoms (n = 10) adsorbed on the doped-defect graphene surface. Initial investigations showed that a single Li atom tends to stabilize at the hollow sites of the graphene lattice [38]. To determine the maximum lithium storage capacity, additional Li atoms were progressively introduced onto the surface of doped-defect graphene (NG1) structure. The theoretical specific capacity was calculated using (3), with NG1 exhibiting the highest capacity of 453.88 mAh $g^{-1}$. These theoretical values are supported by experimental findings, which report exceptionally high capacities of approximately 199 mAh $g^{-1}$ for N-doped graphene and 235 mAh $g^{-1}$ for B-doped graphene at a current density of 25 A $g^{-1}$ corresponding to a full charge time of about 30 seconds [39]. To evaluate structural integrity, the bond lengths of N–C (dopant–carbon) and C–C were measured following the adsorption of ten Li atoms, as summarized in Table 3. For the NG1 structure, only minimal deformation was observed. The average C–C bond length exhibited a slight decrease of approximately 2.09%, while the N–C bond length increased by 4.51% relative to their pristine values. These minor changes indicate that NG1 maintains structural stability under high lithium loading.

Table 3: N-C and C-C bond lengths before and after Li adsorption for NG1.

| Before Adsorption (n = 0) | | | After Adsorption (n = 10) | |
|---|---|---|---|---|
| Structure | d(N-C) | d(C-C) | d(N-C) | d(C-C) |
| NG1 | 1.33 | 1.43 | 1.39 | 1.40 |

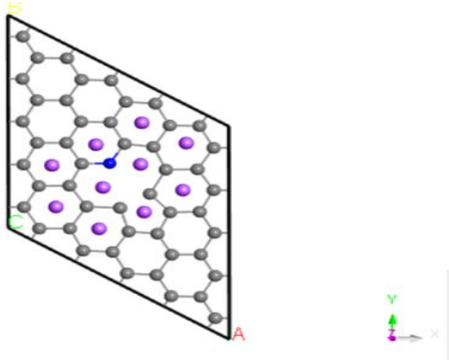

Figure 6: The optimized geometries of ten Li atoms adsorbed on NG1.

# 4 CONCLUSIONS

In this study, comprehensive density functional theory (DFT) calculations were conducted to explore the lithium adsorption, diffusion, and desorption behaviors on pristine graphene, nitrogen-doped graphene, and nitrogen-doped defect graphene. The presence of structural defects was found to significantly enhance lithium adsorption by creating energetically favorable sites. Moreover, nitrogen doping further strengthens the interaction between lithium and the graphene surface.

Among the examined structures, N-doped defect graphene (NG1) exhibited the lowest energy barriers for both lithium diffusion and desorption, suggesting its potential for high-rate charge/discharge performance in lithium-ion batteries (LIBs). The theoretical specific capacity of NG1 was calculated to be as high as 453.88 mAh $g^{-1}$, indicating strong promise for next-generation anode materials. Overall, these findings contribute to a deeper understanding of lithium–graphene interactions and offer a foundation for the rational design of high-capacity, stable anode materials for advanced LIB applications.

# REFERENCES


[1] Y. Morita, Y. Saito, T. Yoshioka, and T. Shiratori, "Estimation of recoverable resources used in lithium-ion batteries from portable electronic devices in Japan," Resources, Conservation and Recycling, vol. 175, p. 105884, 2021.

[2] Z. B. Omariba, L. Zhang, and D. Sun, "Review on health management system for lithium-ion batteries of electric vehicles," Electronics, vol. 7, p. 72, 2018.

[3] Ray, "Novel SiCNW-Si/$SiO_x$-graphite based composite anode materials for Li-ion battery," University of Waterloo, 2018.

[4] L. F. C. Pereira, I. Savić, and D. Donadio, "Thermal conductivity of one-, two-and three-dimensional sp2 carbon," New Journal of Physics, vol. 15, p. 105019, 2013.

[5] P. Bazylewski and G. Fanchini, "1.13-graphene: Properties and applications," Comprehensive Nanoscience and Nanotechnology, vol. 1, pp. 287-304, 2019.

[6] W.-J. Yin, Y.-E. Xie, L.-M. Liu, R.-Z. Wang, X.-L. Wei, and L. Lau, et al., "R-graphyne: A new two-dimensional carbon allotrope with versatile Dirac-like point in nanoribbons," Journal of Materials Chemistry A, vol. 1, pp. 5341-5346, 2013.

[7] C. Neto, F. Guinea, and N. M. Peres, "Drawing conclusions from graphene," Physics World, vol. 19, p. 33, 2006.

[8] M. Liang and L. Zhi, "Graphene-based electrode materials for rechargeable lithium batteries," Journal of Materials Chemistry, vol. 19, pp. 5871-5878, 2009.

[9] P. Guo, H. Song, and X. Chen, "Electrochemical performance of graphene nanosheets as anode material for lithium-ion batteries," Electrochemistry Communications, vol. 11, pp. 1320-1324, 2009.

[10] P. Lian, X. Zhu, S. Liang, Z. Li, W. Yang, and H. Wang, "Large reversible capacity of high quality graphene sheets as an anode material for lithium-ion batteries," Electrochimica Acta, vol. 55, pp. 3909-3914, 2010.

[11] D. Pan, S. Wang, B. Zhao, M. Wu, H. Zhang, and Y. Wang, et al., "Li storage properties of disordered graphene nanosheets," Chemistry of Materials, vol. 21, pp. 3136-3142, 2009.

[12] G. Wang, X. Shen, J. Yao, and J. Park, "Graphene nanosheets for enhanced lithium storage in lithium ion batteries," Carbon, vol. 47, pp. 2049-2053, 2009.

[13] S. Niyogi, E. Bekyarova, M. E. Itkis, J. L. McWilliams, M. A. Hamon, and R. C. Haddon, "Solution properties of graphite and graphene," Journal of the American Chemical Society, vol. 128, pp. 7720-7721, 2006.

[14] C. Uthaisar and V. Barone, "Edge effects on the characteristics of Li diffusion in graphene," Nano Letters, vol. 10, pp. 2838-2842, 2010.

[15] C. Uthaisar, V. Barone, and J. E. Peralta, "Lithium adsorption on zigzag graphene nanoribbons," Journal of Applied Physics, vol. 106, 2009.

[16] M. Khantha, N. Cordero, L. Molina, J. Alonso, and L. Girifalco, "Interaction of lithium with graphene: An ab initio study," Physical Review B – Condensed Matter and Materials Physics, vol. 70, p. 125422, 2004.

[17] X. Wang, Z. Zeng, H. Ahn, and G. Wang, "First-principles study on the enhancement of lithium storage capacity in boron doped graphene," Applied Physics Letters, vol. 95, 2009.

[18] D. Wei, Y. Liu, Y. Wang, H. Zhang, L. Huang, and G. Yu, "Synthesis of N-doped graphene by chemical vapor deposition and its electrical properties," Nano Letters, vol. 9, pp. 1752-1758, 2009.

[19] D. Deng, X. Pan, L. Yu, Y. Cui, Y. Jiang, and J. Qi, et al., "Toward N-doped graphene via solvothermal synthesis," Chemistry of Materials, vol. 23, pp. 1188-1193, 2011.

[20] C. Zhang, L. Fu, N. Liu, M. Liu, Y. Wang, and Z. Liu, "Synthesis of nitrogen-doped graphene using embedded carbon and nitrogen sources," Advanced Materials, vol. 23, pp. 1020-1024, 2011.

[21] L. M. Reddy, A. Srivastava, S. R. Gowda, H. Gullapalli, M. Dubey, and P. M. Ajayan, "Synthesis of nitrogen-doped graphene films for lithium battery application," ACS Nano, vol. 4, pp. 6337-6342, 2010.

[22] Ma, X. Shao, and D. Cao, "Nitrogen-doped graphene nanosheets as anode materials for lithium ion batteries: A first-principles study," Journal of Materials Chemistry, vol. 22, pp. 8911-8915, 2012.

[23] P. Hohenberg and W. Kohn, "Inhomogeneous electron gas," Physical Review, vol. 136, p. B864, 1964.

[24] J. Tirado-Rives and W. L. Jorgensen, “Performance of B3LYP density functional methods for a large set of organic molecules,” Journal of Chemical Theory and Computation, vol. 4, pp. 297-306, 2008.

[25] S. Zavatski, E. Neilande, H. Bandarenka, A. Popov, S. Piskunov, and D. Bocharov, “Density functional theory for doped TiO2: Current research strategies and advancements,” Nanotechnology, vol. 35, p. 192001, 2024.

[26] S. R. Koshkaki, “An overview of Density-Functional-Theory (DFT) for students,” 2015.

[27] J. P. Perdew, K. Burke, and M. Ernzerhof, “Generalized gradient approximation made simple,” Physical Review Letters, vol. 77, p. 3865, 1996.

[28] L. Panchakarla, K. Subrahmanyam, S. Saha, A. Govindaraj, H. Krishnamurthy, and U. Waghmare, et al., “Synthesis, structure, and properties of boron- and nitrogen-doped graphene,” Advanced Materials, vol. 21, pp. 4726-4730, 2009.

[29] H. M. Jeong, J. W. Lee, W. H. Shin, Y. J. Choi, H. J. Shin, and J. K. Kang, et al., “Nitrogen-doped graphene for high-performance ultracapacitors and the importance of nitrogen-doped sites at basal planes,” Nano Letters, vol. 11, pp. 2472-2477, 2011.

[30] P. Wu, Z. Cai, Y. Gao, H. Zhang, and C. Cai, “Enhancing the electrochemical reduction of hydrogen peroxide based on nitrogen-doped graphene for measurement of its releasing process from living cells,” Chemical Communications, vol. 47, pp. 11327-11329, 2011.

[31] G. Kaur, S. Gupta, and K. Dharamvir, “Structures and energetics of lithium adatom and its dimer on graphene – a DFT study,” Applied Surface Science, vol. 334, pp. 19-23, 2015.

[32] S. Mukherjee, L. Kavalsky, and C. V. Singh, “Ultrahigh storage and fast diffusion of Na and K in blue phosphorene anodes,” ACS Applied Materials & Interfaces, vol. 10, pp. 8630-8639, 2018.

[33] G. El Hachimi, J. A. Jiménez-Juárez, C. A. Celaya, D. Sundholm, P. Pyykkö, and J. Muñiz, “Understanding Li interaction in TiO2/graphene composites for high-performance Li-ion battery anodes: A first principles study,” Physica B: Condensed Matter, vol. 660, p. 414878, 2023.

[34] G. Henkelman, B. P. Uberuaga, and H. Jónsson, “A climbing image nudged elastic band method for finding saddle points and minimum energy paths,” The Journal of Chemical Physics, vol. 113, pp. 9901-9904, 2000.

[35] H. Jónsson, G. Mills, and K. W. Jacobsen, “Nudged elastic band method for finding minimum energy paths of transitions,” in Classical and Quantum Dynamics in Condensed Phase Simulations, World Scientific, 1998, pp. 385-404.

[36] S. Jalili and R. Vaziri, “Study of the electronic properties of Li-intercalated nitrogen doped graphite,” Molecular Physics, vol. 109, pp. 687-694, 2011.

[37] J. Zheng, Z. Ren, P. Guo, L. Fang, and J. Fan, “Diffusion of Li+ ion on graphene: A DFT study,” Applied Surface Science, vol. 258, pp. 1651-1655, 2011.

[38] D. Das, S. Kim, K.-R. Lee, and A. K. Singh, “Li diffusion through doped and defected graphene,” Physical Chemistry Chemical Physics, vol. 15, pp. 15128-15134, 2013.

[39] Z.-S. Wu, W. Ren, L. Xu, F. Li, and H.-M. Cheng, “Doped graphene sheets as anode materials with superhigh rate and large capacity for lithium ion batteries,” ACS Nano, vol. 5, pp. 5463-5471, 2011.